POLITECNICO
MILANO 1863

SCUOLA DI INGEGNERIA INDUSTRIALE
E DELL'INFORMAZIONE

Executive Summary of the Thesis

Ising Model with Extended Interactions: Monte Carlo Study of High-Entropy Oxides

Laurea Magistrale in Engineering Physics - Ingegneria Fisica

Author: Lorenzo Guerra

Advisor: Prof. Paolo Biscari

Co-advisors: Prof. Giacomo Claudio Ghiringhelli, Prof. Marco Moretti

Academic year: 2024-2025

1. Introduction

The Ising model is one of the most widely used theoretical frameworks to describe magnetic ordering in condensed matter systems. When extended to include interactions beyond nearest neighbours, it becomes a powerful tool to capture the emergence of complex ordered phases and to study critical phenomena.
In parallel, novel classes of materials, entropy-stabilized oxides and high-entropy oxides, have recently attracted attention due to their high configurational disorder. In 2015, Rost *et al.* [1] quenched an equimolar mixture of MgO, NiO, CuO, CoO and ZnO producing a single-phase rock-salt structure, $(Mg_{0.2}Co_{0.2}Ni_{0.2}Cu_{0.2}Zn_{0.2})O$, where metallic cations were randomly distributed in a face-centred cubic lattice. The authors demonstrated that entropy dominates the thermodynamic landscape for the compound, playing a pivotal role towards stability. The obtained crystal shows antiferromagnetic ordering, where <111> planes are ferromagnetically ordered, and adjacent planes are antiferromagnetically coupled.
Experimental measurements have been performed on $(Mg_{0.2}Co_{0.2}Ni_{0.2}Cu_{0.2}Zn_{0.2})O$ by Jimenez *et. al* [2] and Zhang *et. al* [3] to extrapolate the Néel temperatures, obtaining respectively values of 113 K and 135 K, while Monte Carlo simulations have been performed by Ràk and Brenner [4], and a critical temperature of 170 K was extracted from the peak of the specific heat, while a temperature of 118 K was calculated from a numerical fitting of the paramagnetic behaviour of $c(T)$.

1.1. Contents

The main goal of this thesis work was the characterization (through Monte Carlo methods) of the antiferromagnetic - paramagnetic phase transition, occurring on some realizations of high-entropy oxides.
The system has been described using an extension of the well-known Ising model, where both interactions between nearest-neighbours (NN) and next-nearest-neighbours (NNN) lattice sites was considered.
Before addressing the simulation of HEOs, a characterization of the extended Ising model was carried out by analysing the impact of NNN interactions on square, simple cubic, and FCC lattices. From this analysis, critical temperatures, critical exponents, and low-temperature

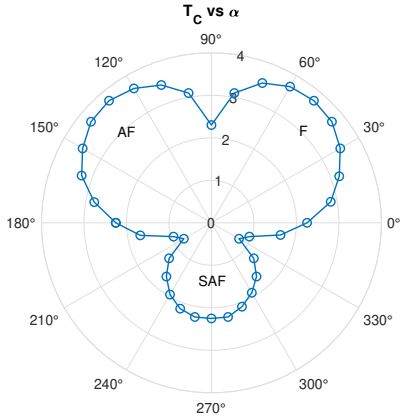

Figure 1: Critical temperatures extracted from the peaks of $c(T)$, square lattice.

ordered phases were determined. In addition, a simple theoretical model was proposed to relate the critical temperatures to the values of the NN and NNN exchange constants introduced in the extended Ising framework.

2. Extended Ising Model

The introduction of next-nearest-neighbour interactions in the Ising model is expressed by the Hamiltonian function shown in the following equation:

$$H = -J_1 \sum_{\langle ij \rangle} s_i s_j - J_2 \sum_{\langle ik \rangle} s_i s_k$$

where the $\langle ij \rangle$ couple identifies spins that are NN, while the $\langle ik \rangle$ couple spins that are NNN. To simulate the effect of different values for J_1 and J_2, these exchange parameters have been defined as follows:

$$\begin{cases} J_1 = Jcos(\alpha) \\ J_2 = Jsin(\alpha) \end{cases}$$

and each lattice geometry has been analysed exploring values of α from $-180°$ to $180°$, with steps of $\Delta\alpha = 10°$

2.1. Square lattice

From the peaks of the specific heat it is possible to extract the critical temperature as a function of α, and the results are displayed in Figure 1. Three qualitatively different sections of the polar plot are clearly visible (F, AF and SAF), and each of them corresponds to a different low-temperature configuration, all characterized and shown in Figure 2. It is possible to calculate

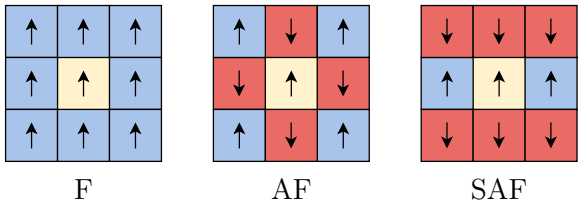

Figure 2: Ordered configurations for F, AF and SAF phases.

the energy density associated with each ordered phase (that is, given Figure 2, the energy corresponding to the interaction of the central spin with all its NN and NNN neighbours). By relating this quantity to α, one can predict the fundamental state and identify the angular values in which the configurations are degenerate. F and AF are degenerate at 90°, AF and SAF at approximately $-153°$ and SAF and F at approximately 27°. The behaviour of the energy densities associated to the three different configurations is directly related to the trend observed in Figure 1: the lower is the energy of the fundamental state for a given α, the higher is the critical temperature observed, and this is an effect of frustration, which is present only in the SAF phase. Given the well-known value of the critical temperature for the 2D Ising model found by Onsager, that is $T_C \approx 2.3J$, through numerical fitting between the energy densities and the critical temperatures, an "effective value" for the exchange constant has been found, that is $J = -u/3.7$ for the non-frustrated phases (F and AF), and $J = -u/4.2$ for the frustrated phase (SAF).

2.2. Simple cubic lattice

The same procedure described in section 2.1 has been performed on a 3D simple cubic lattice described by the extended Ising model. In Figure 3 are reported the critical temperatures, where four different phases can be seen, one pertaining ferromagnetic ordering (F), one *G-type antiferromagnetism*, one *C-type antiferromagnetism* and one *A-type antiferromagnetism*, all depicted in Figure 4. From the values of the energy densities associated to the ordered configurations, it has been found that:

- F and G are degenerate for $\alpha = 90°$;
- G and C are degenerate for $\alpha \approx 194°$;
- C and A are degenerate for $\alpha = -90°$;

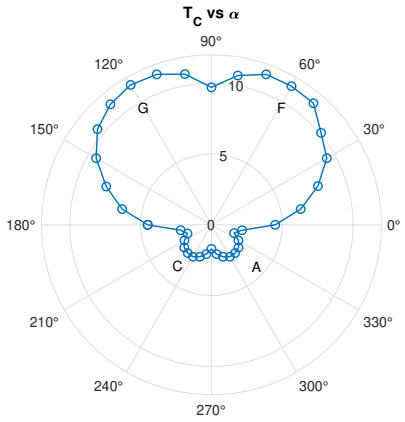

Figure 3: Critical temperatures extracted from the peaks of $c(T)$, simple cubic lattice.

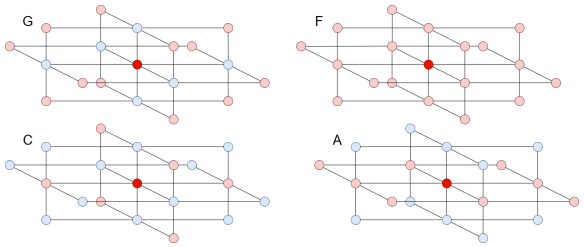

Figure 4: Ordered configurations for F, G, C and A phases.

- A and F are degenerate for $\alpha \approx -14°$;

To obtain the value of the effective exchange constant the established numerical result for the critical temperature of the 3D Ising model was used, that is $T_C \approx 4.5J$, and the values for the effective exchange constant has been found, through numerical fitting, to be $J = -u/5.4$ for the non-frustrated phases (F and G) and $J = -u/8.0$ for the frustrated phases (C and A).

2.3. Face-centred cubic lattice

For what concerns FCC lattices, in Figure 5 are depicted the critical temperatures. At first sight, only three phases seem present, however a deeper analysis shows that there are actually four different ordered configurations at low temperatures, one ferromagnetic (F), and three antiferromagnetic (AF1, AF2 and AF3), it is possible to see them depicted in Figure 6. From the analysis of the energy densities, it is found that:

- FM and AF1 are degenerate at $\alpha = -45°$;
- AF1 and AF2 are degenerate at $\alpha \approx -153°$;
- AF2 and AF3 are degenerate at $\alpha = 180°$;
- AF3 and AF1 are degenerate at $\alpha = 90°$.

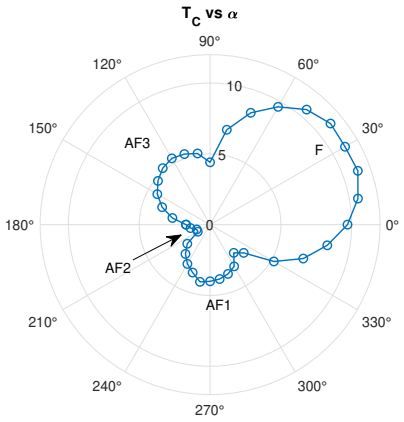

Figure 5: Critical temperatures extracted from the peaks of $c(T)$, FCC lattice.

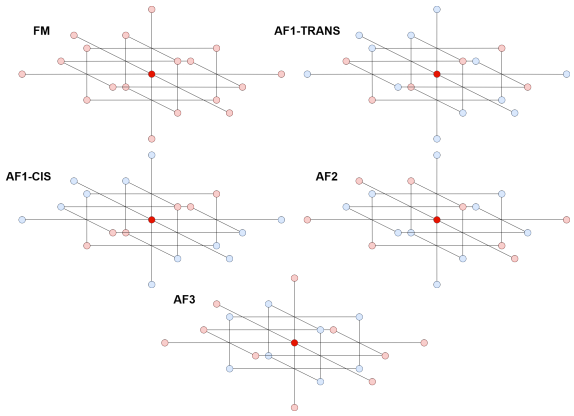

Figure 6: Ordered configurations for F, AF1, AF2 and AF3 phases. AF1 shows two distinguishable degenerate configurations.

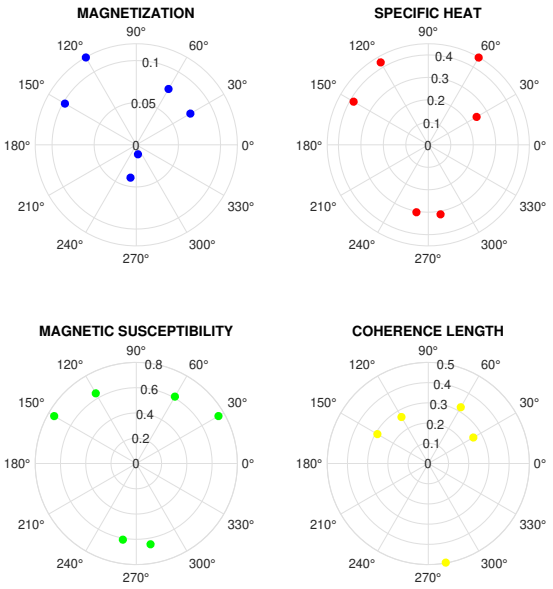

Figure 7: Critical exponents, square lattice

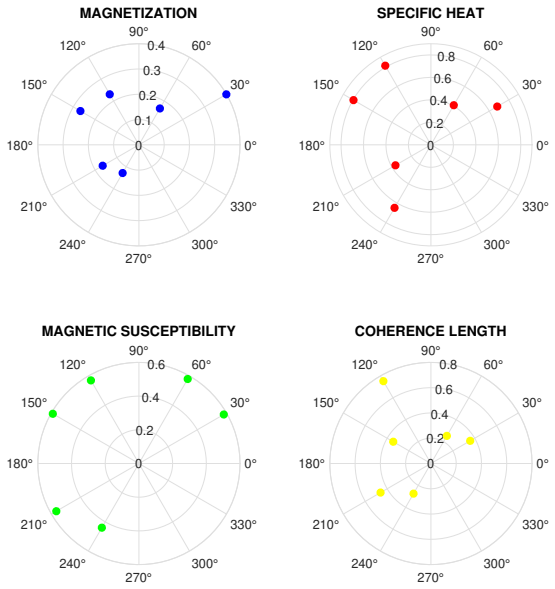

Figure 8: Critical exponents, simple cubic lattice

2.4. Critical exponents

From Monte Carlo data it is possible to recover the critical behaviours of physical quantities such as the magnetization, specific heat, magnetic susceptibility and coherence length. Through numerical fitting, the values for those exponents have been extracted, pertaining some values of α in square and simple cubic lattices. Results are depicted in Figures 7 and 8.
Statistical analysis regarding standard errors for the numerical estimators of the critical exponents brings satisfactory results of "signal-to-noise ratios" of the order $10^1 - 10^2$. The estimated values of the critical exponents result heavily influenced by the right choice of the critical temperature that enters in the fitting model, and its estimate is critical for achieving a correct description of the critical phenomena. In this thesis work, to obtain a punctual estimation for T_C, an iterative procedure has been performed, based on multiple different numerical fitting. As a reference value it has been chosen the simulated temperature correspondent to the maximum value of $c(T)$. Starting from it, an interval between 90% and 110% of this value has been considered, and from it 100 different candidates for T_C were used as parameters in the estimation of critical exponents, and 100 different regressions have been performed. As an estimate for T_C it has been taken the value that maximized R^2 for the fitted model.

3. High-entropy oxides

Simulations of high-entropy oxides were carried out on systems with different cationic compositions. The reference case was the equimolar compound $(Mg_{0.2}Co_{0.2}Ni_{0.2}Cu_{0.2}Zn_{0.2})O$. Additional Monte Carlo data were obtained for structures in which one metallic species was removed:

- A $\rightarrow (Mg_{0.2}Co_{0.2}Ni_{0.2}Cu_{0.2}Zn_{0.2})O$;
- B $\rightarrow (Mg_{0.25}Ni_{0.25}Cu_{0.25}Zn_{0.25})O$;
- C $\rightarrow (Mg_{0.25}Co_{0.25}Cu_{0.25}Zn_{0.25})O$;
- D $\rightarrow (Mg_{0.25}Co_{0.25}Ni_{0.25}Zn_{0.25})O$;
- E $\rightarrow (Co_{0.25}Ni_{0.25}Cu_{0.25}Zn_{0.25})O$ and $(Mg_{0.25}Co_{0.25}Ni_{0.25}Cu_{0.25})O$.

E represents 2 different realizations, since both Mg^{2+} and Zn^{2+} show a null value of the spin quantum number, and the configurations are magnetically equivalent. The exchange constants adopted for both nearest-neighbour (NN) and next-nearest-neighbour (NNN) interactions were taken from the work of Ràk and Brenner [4] (Table 1), and their values depend on the specific pair of interacting atoms.

3.1. Critical temperatures

Due to the stochastic occupation of lattice sites by different metallic cations, a high number of simulations have been conducted to characterize the antiferromagnetic - paramagnetic phase transition. The mean critical temperatures obtained by an ensemble of 50 realizations of the system are visible in Table 2. Errors σ_{T_C} are es-

	Co-Co	Ni-Ni	Cu-Cu	Co-Ni	Co-Cu	Ni-Cu
$\mathbf{J_1}$	0.57	0.83	7.14	0.89	3.58	1.7
$\mathbf{J_2}$	-5.29	-9.47	-18.51	-6.39	-9.11	-10.83

Table 1: Exchange interaction for HEOs, calculated by Ràk and Brenner [4], in units of meV.

	A	B	C	D	E
$\mathbf{T_C}$ **[K]**	160	109	120	146	214
$\sigma_{\mathbf{T_C}}$ **[K]**	3.9	4.1	4.3	4.4	2.8

Table 2: Critical temperatures for different HEO compositions, result of 50 different simulations for each composition.

timated through the standard deviations for the T_Cs extracted for the ensemble.
The experimental values for T_C available in literature for the compound *A* are 113 K [3] and 135 K [2], while Monte Carlo simulations [4] brought values of 170 K and 118 K. The values obtained in this thesis work are compatible with the numerical extrapolations made by Ràk and Brenner, but overestimate the experimental results.

3.2. Low-temperature configurations

To characterize the antiferromagnetic – paramagnetic phase transition, an order parameter different from the conventional magnetization must be employed. In the first part of the thesis work, the *Edwards–Anderson order parameter* was used, showing clear transitions in correspondence to the peaks in the specific heat. Subsequently, after determining the low-temperature configurations corresponding to the two degenerate AF1 phases (described in Section 2.3 and shown in Figure 6), explicit expressions were derived for eight different staggered magnetizations: four associated with the *cis* configuration and four with the *trans* configuration.

3.3. Domains formation

The low-temperatures values taken by those magnetization enabled the identification of domains formation: lower-than-expected values are indicators of the fact that the magnetization of the lattice is not fully coherent, and at some point a domain wall has disrupted long-range magnetic ordering. An example is given in Figure 9, where several points are well below the saturated magnetization per spin (equal to 2 in this case). The same behaviour has been observed for the compound B. It is possible to explain this phenomena describing the *average energy density* associated to the ordered configurations of HEOs. Considering an average value for NN and NNN exchange constants ($\bar{J}_1$ and $\bar{J}_2$), their expression is:

$$\bar{J} = \sum_{ij\ couples} J_{ij} \cdot S_i S_j \cdot N_i N_j,$$

where $N_{i(j)}$ is the concentration and $S_{i(j)}$ the spin quantum number of the i-th (j-th) species, while J_{ij} the exchange constant. Considering the ordered configurations displayed in Figure 6, one can find the expression of the energy density $u = 6\bar{J}_2$ associated to the AFM1 phases. Using the values for *J*s calculated by Ràk and Brenner it is possible to demonstrate that the compounds B and C are the two showing a considerably lower value for this *averaged energy density* (Table 3).

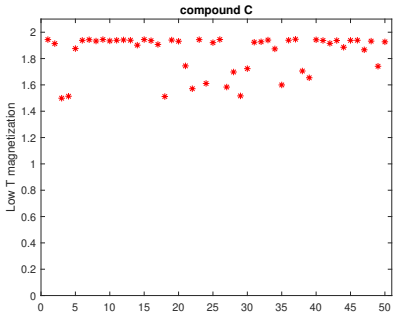

Figure 9: Low temperature magnetizations for the 50 realizations of compound C

	A	B	C	D	E
$\mathbf{u}$ **[meV]**	-11.5	-7.32	-8.76	-11.6	-17.9

Table 3: Averaged energy densities for HEOs realization, considering the definitions of average exchange constants.

3.4. Measured exchange constant

Other simulations have been carried out using different values of the exchange constants,

	Ni-Ni	Cu-Cu	Co-Ni	Co-Cu	Ni-Cu
$\mathbf{J_2}$	-23.9	-96.5	-3.4	-9.3	-11.6

Table 4: Exchange interaction for HEOs, results of RIXS measurements, in units of meV.

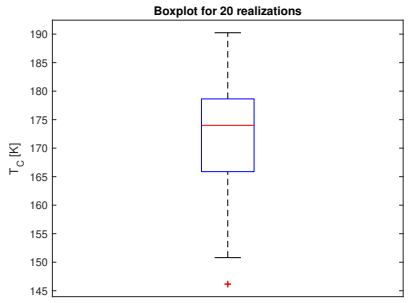

Figure 10: Boxplot showing 20 different T_C obtained with $J_2^{Co-Co} = 0$.

hoping to find better agreements between the Néel temperature obtained through Monte Carlo simulations and experimental measurements. These new values were obtained through RIXS measurement at the ESRF facility in Grenoble (France) and only describe NNN coupling. Those values are reported in Table 4. Unfortunately, it was not possible to retrieve values regarding the interaction between cobalt - cobalt couples of next-nearest-neighbours spins.
Even considering $J^{Co-Co} = 0$ however, it was not possible to obtain Néel temperatures closer to those reported in literature. In Figure 10 it is possible to see the statistical distributions of 20 T_Cs obtained for the compound A, using the new values for the exchange constants. The mean value of 175 K is even further from experimental data reported in [2] and [3].

4. Conclusions

From the preliminary analysis of ordered systems described by the extended Ising model, including both NN and NNN interactions, critical temperatures and low-temperature ordered phases were extracted. By combining these results, a simple yet effective model was developed, relating the energy density of a given configuration to its critical temperature. Numerical fitting then allowed the calculation of an effective exchange constant.

Monte Carlo data were also used to extrapolate the values of the critical exponents, associated with the critical behaviour of magnetization, specific heat, magnetic susceptibility, and coherence length. Although the statistical estimators of the exponents showed relatively low standard errors, leading to a large signal-to-noise ratio, the accuracy of the estimation was found to be highly sensitive to the choice of the critical temperature, which must therefore be determined with particular care.
The simulations conducted on HEOs brought numerical values for the Néel temperatures well above the experimental values. The intrinsic limits of the Ising model could be the main reason for these discrepancies: true HEOs are in fact described by the Heisenberg model, for which the Ising model constitutes only an approximation. Between those two descriptions the Ising model, due to its constraints, tends to overestimate the strength of magnetic ordering and the critical temperatures.

References

[1] Christina M Rost, Edward Sachet, Trent Borman, Ali Moballegh, Elizabeth C Dickey, Dong Hou, Jacob L Jones, Stefano Curtarolo, and Jon-Paul Maria. Entropy-stabilized oxides. *Nature communications*, 6 (1):8485, 2015.

[2] Marco Polo Jimenez-Segura, Tomohiro Takayama, David Bérardan, Andreas Hoser, Manfred Reehuis, Hidenori Takagi, and Nita Dragoe. Long-range magnetic ordering in rocksalt-type high-entropy oxides. *Applied Physics Letters*, 114(12):122401, 03 2019.

[3] Junjie Zhang, Jiaqiang Yan, Stuart Calder, Qiang Zheng, Michael A McGuire, Douglas L Abernathy, Yang Ren, Saul H Lapidus, Katharine Page, Hong Zheng, et al. Long-range antiferromagnetic order in a rocksalt high entropy oxide. *Chemistry of Materials*, 31(10):3705–3711, 2019.

[4] Zs Rák and DW Brenner. Exchange interactions and long-range magnetic order in the (mg, co, cu, ni, zn) o entropy-stabilized oxide: A theoretical investigation. *Journal of Applied Physics*, 127(18), 2020.